Direct Detection and Kinetic Analysis of Covalent Intermediate Formation in the 4-Amino-4-deoxychorismate Synthase Catalyzed Reaction

Ze He[‡] and Michael D. Toney*[,§]

Department of Chemistry, Central Connecticut State University, 1615 Stanley Street, New Britain, Connecticut 06050, and Department of Chemistry, University of California—Davis, Davis, California 95616

Received October 31, 2005; Revised Manuscript Received February 13, 2006

ABSTRACT: Chorismate-utilizing enzymes catalyze diverse reactions, providing critical physiological functions unique to plants, bacteria, fungi, and some parasites. Their absence in animals makes them excellent targets for antimicrobials and herbicides. 4-Amino-4-deoxychorismate synthase (ADCS) catalyzes the first step in folate biosynthsis and shares a common core mechanism with isochorismate synthase (IS) and anthranilate synthase (AS), in which nucleophile addition at C2 initiates these reactions. Evidence was presented previously [He, Z., Stigers Lavoie, K. D., Bartlett, P. A., and Toney, M. D. (2004) *J. Am. Chem. Soc*. *126*, 2378−2385] that K274 is the nucleophile in ADCS, implying formation of a covalent intermediate. Herein, we report the direct detection of this covalent intermediate formed in ADCS-catalyzed reactions by ESI-MS. Difference spectra show the covalent intermediate has an absorption maximum at 310 nm. This was used to study the pre-steady-state kinetics of covalent intermediate formation under various conditions. Additionally, E258 in ADCS was shown to be critical to formation of the covalent intermediate by acting as a general acid catalyst for loss of the C4 hydroxyl group. The E258A/D mutants both exhibit very low activity. Acetate is a poor chemical rescue agent for E258D but an excellent one for E258A, with a 20000-fold and 3000-fold rate increase for Gln-dependent and NH_4^+-dependent activities, respectively. Lastly, A213 in IS (structurally homologous to K274 in ADCS) was changed to lysine in an attempt to convert IS to an ADCS-like enzyme. HPLC studies support the formation of a covalent intermediate with this mutant.

4-Amino-4-deoxychorismate synthase (ADCS) is a key enzyme in folate biosynthesis. Tetrahydrofolate and its derivatives, commonly referred as folates, are a group of vital cofactors for enzymes that catalyze one-carbon transfers. Folates carry and donate one-carbon units in numerous metabolic processes such as photorespiration in plants and the biosynthesis of methionine (*1*). They are also involved in DNA biosynthesis with implications for the regulation of gene expression, chromatin structure, genomic repair, and genomic stability (*2*). In microorganisms and plants, folates are synthesized de novo from pterin, glutamate, and *p*-aminobenzoate (PABA).

ADCS catalyzes the first step of PABA biosynthesis, which starts from chorismate. It adds ammonia, generated by enzymatic (PabA) hydrolysis of glutamine, to chorismate, generating 4-amino-4-deoxychorismate (ADC). ADC is then acted on by 4-amino-4-deoxychorismate lyase (ADCL) to give PABA (*3*−*5*). The latter is subsequently incorporated into folates by dihydropteroate synthase (DHPS) as shown in Figure 1.

ADCS has been suggested to share an evolutionary relationship with other chorismate-utilizing enzymes because of their sequence homology, structural similarity, and the similarity of the reactions they catalyze. This group of enzymes includes anthranilate synthase (AS) (*6*), isochorismate synthase (IS) (*7*), PapA (*8*), PhzE (*9*), and Irp9 (*10*). Figure 2 shows the entire family of chorismate-utilizing enzymes, including the two structurally unrelated enzymes chorismate mutase (CM) (*11*) and chorismate lyase (CL) (*12*). Chorismate-utilizing enzymes are responsible for producing a number of carbocylic aromatic compounds that are critical to the survival of plants, bacteria, fungi, and apicomplexan parasites (*13*, *14*). This pathway is unique to these organisms and, thus, is an attractive target for antibiotics and herbicides.

The sequence homology and structural similarity displayed among this group of chorismate-utilizing enzymes imply a common chemical mechanism. Several different proposals have been investigated (*15*, *16*) but only recently was a unifying mechanism demonstrated (Figure 3) (*17*). According to this mechanism, AS, IS, and ADCS all initiate replacement of the C4 hydroxyl group by addition of a nucleophile to C2 of chorismate via a S_N2'' displacement reaction. IS uses water, AS uses ammonia, and ADCS uses the ϵ-amino group of K274 as nucleophiles. In the IS reaction, the initial C2 adduct is directly released from the enzyme active site as the product isochorismate. In the AS reaction, the 2-amino-2-deoxyisochorismate (ADIC) intermediate is tightly bound to the active site, which subsequently catalyzes pyruvate elimination. ADIC was identified as an intermediate using mutant AS enzymes whose elimination reactions were disrupted (*18*). In the ADCS reaction, a covalent intermediate

* Corresponding author. Tel: 530-754-5282. Fax: 530-752-8995. E-mail: mdtoney@ucdavis.edu.
[‡] Central Connecticut State University.
[§] University of California—Davis.

10.1021/bi052216p CCC: $33.50
Published on Web 03/22/2006

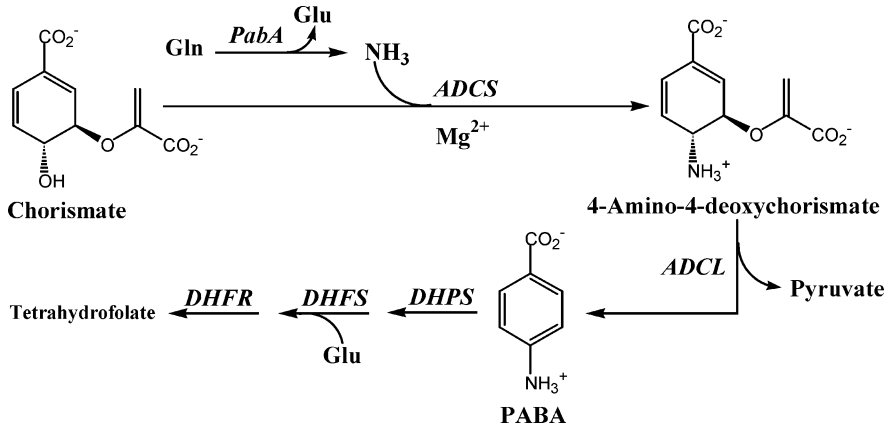

FIGURE 1: Folate biosynthesis in plants, bacteria, fungi, and *P. falciparum* parasites. 4-Amino-4-deoxychorismate synthase (ADCS) catalyzes the amination of chorismate at C4.

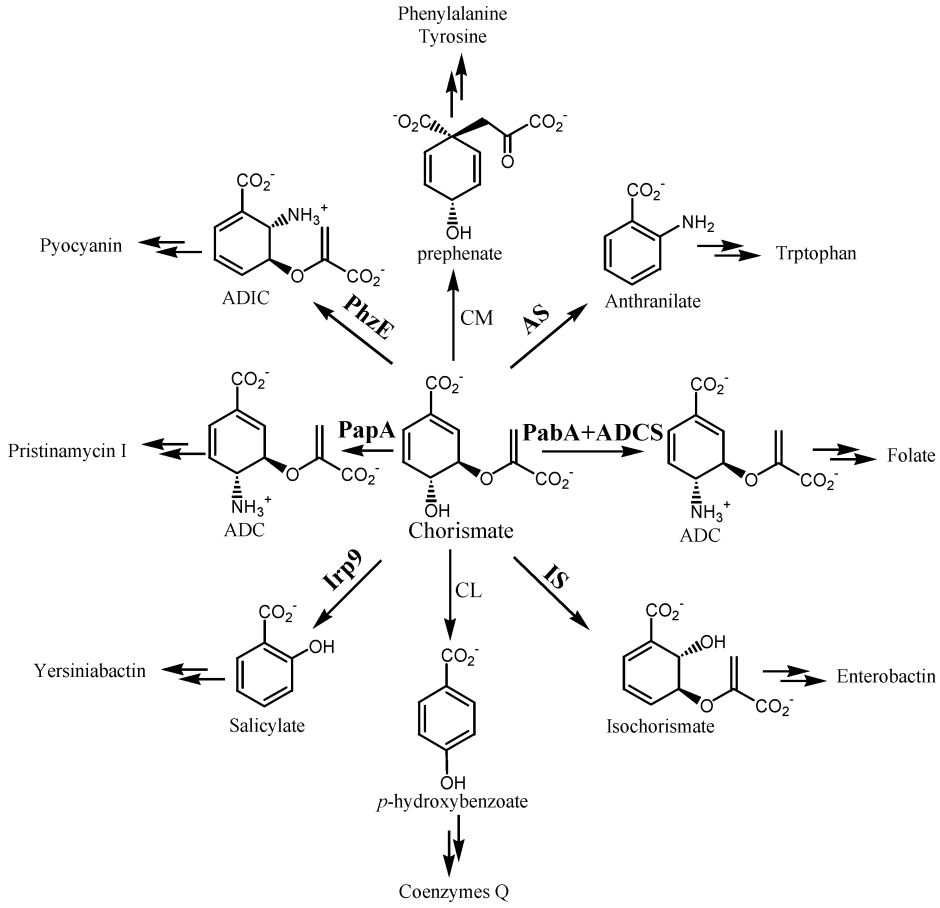

FIGURE 2: Overview of chorismate-dependent pathways. Abbreviations: AS (anthranilate synthase), ADCS (4-amino-4-deoxychorismate synthase), IS (isochorismate synthase), CM (chorismate mutase), and CL (chorismate lyase). The enzymes shown in bold are structurally homologous. The end product of each pathway is given.

with K274 is formed, which is converted to ADC by reverse S_N2'' addition of ammonia to C4. A recent electrospray mass spectrometry (ESI-MS) study has shown that 2-fluorochorismate forms a stable covalent adduct with K274 of ADCS, which irreversibly inhibits the activity of ADCS (*19*). This finding not only explains the antibacterial properties of 6-fluoroshikimate, the precursor of 2-fluorochorismate, but also provides strong evidence for covalent intermediate formation between the true substrate chorismate and K274.

In this study, we demonstrate formation of a covalent adduct between chorismate and K274 of ADCS using ESI-MS. Spectroscopic experiments show an absorption band centered at 310 nm for the covalent intermediate, which enabled the measurement of pre-steady-state kinetics of its formation. We also show that E258 of ADCS is critical to the formation of the covalent intermediate and that acetate can partially restore the activity of the E258A mutant. Finally, we mutated A213 in IS to lysine to convert IS to an ADCS-like enzyme. HPLC data provide evidence supporting formation of a covalent intermediate in the A213K mutant.

EXPERIMENTAL PROCEDURES

Materials. Chorismic acid (barium salt), PABA, anthranilic acid, NADH, Bicine, DTT, isopropyl β-D-thiogalactopyra-

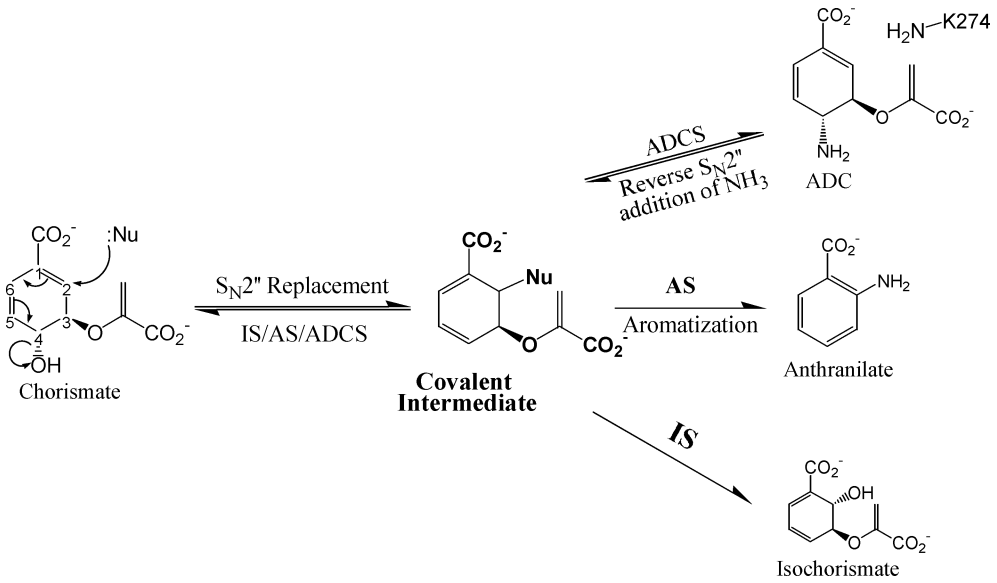

FIGURE 3: Common mechanism employed by the three homologous chorismate-utilizing enzymes IS, AS, and ADCS. The ring carbon numbers are shown for chorismate. All three enzymes catalyze their reactions via a common intermediate, which is generated by addition of a nucleophile to C2 and elimination of the C4 hydroxyl group. AS and IS both employ exogenous nucleophiles, while ADCS uses the ϵ-amino group of K274 and thus affords a covalent intermediate.

noside (IPTG), pyridoxal 5′-phosphate (PLP), 6-diazo-5-oxo-L-norleucine (DON), sodium acetate, ammonium sulfate, magnesium chloride, and manganese chloride were from Sigma-Aldrich. Lactate dehydrogenase (LDH) was purchased from Roche. All reagents used were of analytical grade. Restriction enzymes and DNA ligase were from New England Biolabs. Taq DNA polymerase was from Promega. Primers were synthesized by Invitrogen.

Enzyme Preparation. The genes for PabA, ADCS, and ADCL were cloned from *Escherichia coli* K12 chromosomal DNA (*17*). The PabA gene was subcloned into the pET3a vector (Novagen) using the *Nde*I and *Bam*HI restriction sites. ADCS and ADCL genes were subcloned using the *Nde*I and *Bam*HI restriction sites into the pET28a vector (Novagen) for expression as a His_6-tagged fusions. Overexpression and purification of these enzymes were carried out as described (*17*).

Mutations were introduced into the pET28a-*pabB* construct using the QuikChange site-directed mutagenesis kit (Stratagene). K274A and K274R were constructed, overexpressed, and purified as described (*17*). The E258A mutagenic primers were 5′-GGTGCAATTTTAAGCCTTTCGCCAGCGCGGTTTATTCTTTGTG-3′ (forward) and 5′-CACAAAGAATAAACCGCGCTGGCGAAAGGCTTAAAATTGCACC-3′ (reverse). The E258D mutagenic primers were 5′-GGTGCAATTTTAAGCCTTTCGCCAGATCGGTTTATTCTTTGTG-3′ (forward) and 5′-CACAAAGAATAAACCTATCTGGCGAAAGGCTTAAAATTGCACC-3′ (reverse). E258A and E258D were overexpressed and purified in a fashion similar to that of the wild-type enzyme.

The *entC* gene encoding IS was amplified from *E. coli* BL21(DE3) chromosomal DNA using Taq DNA polymerase. Chromosomal DNA was prepared by boiling cells in water for 10 min. The primers used for PCR were designed to introduce *Nde*I and *Bam*HI restriction sites into the PCR products. Their sequences were 5′-GCGCGGCAGCCATATGGATACGTCACTGGCTGAGGAAG-3′ (forward) and 5′-CATGTTGAACGTTTTTGGATTGCATTAAGGATCCGAATTC-3′ (reverse). The *entC* gene was cloned using the *Nde*I and *Bam*HI restriction sites into the pET28a vector for expression as a His_6-tagged fusion.

Overexpression and purification of IS were carried out as follows. BL21(DE3) Gold cells harboring the pET28a-*entC* construct were grown in TB medium at 37 °C. Overproduction was induced by addition of IPTG to 0.5 mM at OD_{600} = 0.5. Incubation continued for an additional 18 h at 20 °C. The cells were harvested, and the pellet was resuspended in lysis buffer (50 mM NaH_2PO_4, 300 mM NaCl, 10 mM imidazole, 1 mM β-mercaptoethanol, 5 mM $MgCl_2$, 0.5 mg/mL lysozyme, 0.2 unit/mL DNase I, pH 7.4). Cells were chilled on ice and disrupted by sonication. Cell debris was pelleted by centrifugation at 15000 rpm for 45 min. The supernatant was incubated at 4 °C for 60 min with NTA-Ni resin (Qiagen). The resin was loaded into a column and washed with 15 bed volumes of wash buffer (50 mM NaH_2PO_4, 300 mM NaCl, 20 mM imidazole, 1 mM β-mercaptoethanol, 5 mM $MgCl_2$, pH 7.4). Bound protein was eluted with a linear 0.6 L 20−300 mM imidazole gradient in 50 mM NaH_2PO_4, 300 mM NaCl, 1 mM β-mercaptoethanol, and 5 mM $MgCl_2$, pH 7.4. Activity was determined with the spectrophotometric assay (described in Spectrophotometric Activity Assays). Active fractions were pooled, concentrated, and analyzed by SDS−PAGE. The final protein sample was dialyzed against 20 mM KP_i, 50 mM KCl, and 1 mM DTT, pH 7.4, and stored at −80 °C. The overall yield was ~3 mg of IS/g of cell paste.

For the A213K mutant IS, the mutation was introduced into the pET28a-*entC* construct using the QuikChange site-directed mutagenesis kit. The IS A213K mutagenic primers were 5′-GCTCCATTCCGTTAAAAGGTTCCGCGCGTCGTCAGCCG-3′ (forward) and 5′-CGGCTGACGACGCGCGGAACCTTTTAACGGAATGGAGC-3′ (reverse). The mutant was overexpressed and purified similarly to the wild-type IS enzyme.

Mass Spectral Analysis. Since ESI-MS is salt sensitive and covalent intermediate formation is reversible, ADCS was

exchanged into water immediately prior to mass spectral analysis. A 3K MWCO Centricon concentrator was used. Chorismate used for MS analysis was further purified from the commercial sample using a Waters μBondaPak preparatory C18 column and the HPLC protocol described in the HPLC Analysis section. Purified chorismate collected from the HPLC was lyophilized and reconstituted in water. Base was added to adjust the pH of chorismate solution to 7−8.

A reaction mixture containing 500 μM ADCS, 250 μM $MnCl_2$, and 1 mM chorismate was incubated at room temperature for 5 min before it was diluted with an equal volume of 30% methanol/1% formic acid. Mn^{2+} was used instead of Mg^{2+} because of its lower binding constant. The sample was then directly infused to the spray source on an ABI/Sciex Qstar mass spectrometer with a syringe pump at 5 μL/min flow rate. The source voltage was 4500 V. The ABI BioAnalyst with the Bayesian peak reconstruction tool was used to analyze the data.

Spectrophotometric Activity Assays. Enzyme activity assays for ADCS were based on previously described methods (*3*, *20*). The first assay employs fluorescence detection of PABA (excitation at 290 nm, emission at 340 nm) extracted from reaction mixtures containing ADCL as a coupling enzyme and was used for reactions in which the enzyme activity was low, such as the E258 mutant of ADCS. The second assay couples pyruvate formation in the ADCL reaction to the LDH reaction, monitoring the decrease in NADH absorbance at 340 nm. A standard glutamine-dependent assay contains 100 mM Bicine, pH 8.5, 20 mM glutamine, 5 mM $MgCl_2$, 20 μM PLP, 10 μM ADCL, 200 μM NADH, 4 units/mL LDH, and equimolar ADCS and PabA. A standard NH_4^+-dependent assay contains 100 mM Bicine, pH 8.5, 100 mM $(NH_4)_2SO_4$, 5 mM $MgCl_2$, 20 μM PLP, 10 μM ADCL, 200 μM NADH, and 4 units/mL LDH. Ba^{2+} in the commercial chorismate was always removed by addition of a slight excess of K_2SO_4 before use. EDTA (1 mM) was included in experiments designed to be free of metal ions. All assays were performed at 25 °C.

The activity assay for IS directly monitors the formation of isochorismate by the absorbance increase at 278 nm ($\Delta\epsilon_{\text{isochorismate-chorismate}} = 10211\ M^{-1}\ cm^{-1}$) (*18*). The standard assay contains 50 mM triethanolamine (TEA), pH 7.8, and 5 mM $MgCl_2$. All assays were performed at 25 °C.

Difference Spectral Studies. An HP 8453 diode array spectrophotometer and a split cuvette were used. Enzyme and substrate solutions were initially separated in the two chambers of the split cuvette. A blank spectrum was taken with the solutions unmixed. The difference spectrum was taken immediately after mixing the two solutions, which gives the spectral change incurred by mixing the enzyme and substrate. A standard assay for difference spectral studies contained 50 mM TEA, pH 7.8, 5 mM $MgCl_2$, 1 mM DTT, 10 μM ADCS (with or without equimolar PabA), and 150 μM chorismate. Glutamine was added to 20 mM, and $(NH_4)_2SO_4$ was added to 100 mM if an ammonia source was included. All experiments were perfomed at 25 °C. TEA buffer was used since its absorption does not overlap with that of the covalent intermediate. The k_{cat} value for ADCS at pH 7.8 in TEA buffer is 95% of that at the optimum of pH 8.5.

DON-inactivated PabA was prepared as follows. A 1:1 PabA/ADCS complex was incubated with 25 equiv of DON in 50 mM TEA, pH 7.8, and 5 mM $MgCl_2$ at 25 °C for 20 min. PabA is not alkylated and inactivated by DON unless ADCS is present (*21*). Dialysis was then performed to remove excess DON.

Stopped-Flow Kinetic Analysis. All experiments were performed on an Applied Photophysics SX.18MV-R stopped-flow spectrometer. The covalent intermediate formation was monitored by its absorbance at 310 nm. ADCS (10 μM, with or without equimolar PabA) was mixed against various concentrations of chorismate (with or without 200 mM NH_4^+ as cosubstrate) in 50 mM TEA, pH 7.8, and 5 mM $MgCl_2$ at 25 °C. Averages of four to five traces were used. The background absorbance changes generated by mixing buffer and chorismate were also subtracted for each chorismate concentration. The data were analyzed with Specfit (Spectrum Software Associates).

HPLC Analysis. A standard reaction mixture for HPLC analysis contained 100 mM Bicine, pH 8.5, 5 mM $MgCl_2$, with or without 100 mM $(NH_4)_2SO_4$, 5 mM chorismate or ADC, and 15 μM wild-type IS or its mutant A213K. After 4 h incubation at room temperature, glacial acetic acid was added to 5% to the mixture to lower the pH to 5. The samples were ultrafiltered to remove protein(s) and injected. A Rainin Microsorb-MV analytical C18 column was used to separate reaction mixtures on an Agilent 1100 HPLC system. Isocratic elution with 95% solvent A (5% acetic acid in water) and 5% solvent B (acetonitrile) was employed, and the absorbance at 280 nm was monitored. Peaks were identified by comparing retention times and UV absorption spectra with authentic standards.

ADC was prepared as described (*22*). A reaction mixture containing 30 mM chorismate, 200 mM NH_4HCO_3, pH 8.6, 100 mM $(NH_4)_2SO_4$, 1 mM $MgCl_2$, and 15 μM ADCS was incubated at 37 °C for 3 h. The reaction was quenched with 2.4 mL of chloroform. The aqueous layer was removed and acidified with 2 M trifluoroacetic acid to pH 1. Chloroform (2.4 mL) was initially used to extract chorismic acid, with three portions of 2.4 mL ethyl acetate to complete the extraction. The final aqueous layer was lyophilized and stored at −80 °C. ADC was quantitated using $\epsilon_{272nm} = 5230\ M^{-1}\ cm^{-1}$ (*23*).

RESULTS

Covalent Intermediate Detection. The covalent intermediate formed in the ADCS reaction with chorismate was directly detected by ESI-MS (Figure 4). ADCS alone exists in two forms (Figure 4A). Peaks 1 and 3 are the two main species with a 178 Da mass difference due to an α-N-6-phosphogluconoylated His tag from expression in *E. coli* (*24*). Peaks 2, 4, and 5 are the potassium adducts of the main species, which are also present in Figure 4B−D. On addition of 2 equiv of chorismate and 0.5 equiv of Mn^{2+}, a third major species, peak 6 in Figure 4B, with a 208 Da mass increase from peak 3 appeared in the mass spectrum. This is the mass shift expected from formation of the covalent intermediate between chorismate and K274. Peak 4 in Figure 4B is also 208 Da greater in mass than peak 1 and is interpreted to be the covalent intermediate formed from peak 1, which coincidentally overlaps with the potassium adduct of peak 3.

K274A alone also exists in two forms, as shown in Figure 4C, with a 178 Da mass difference similar to wild type. Peaks

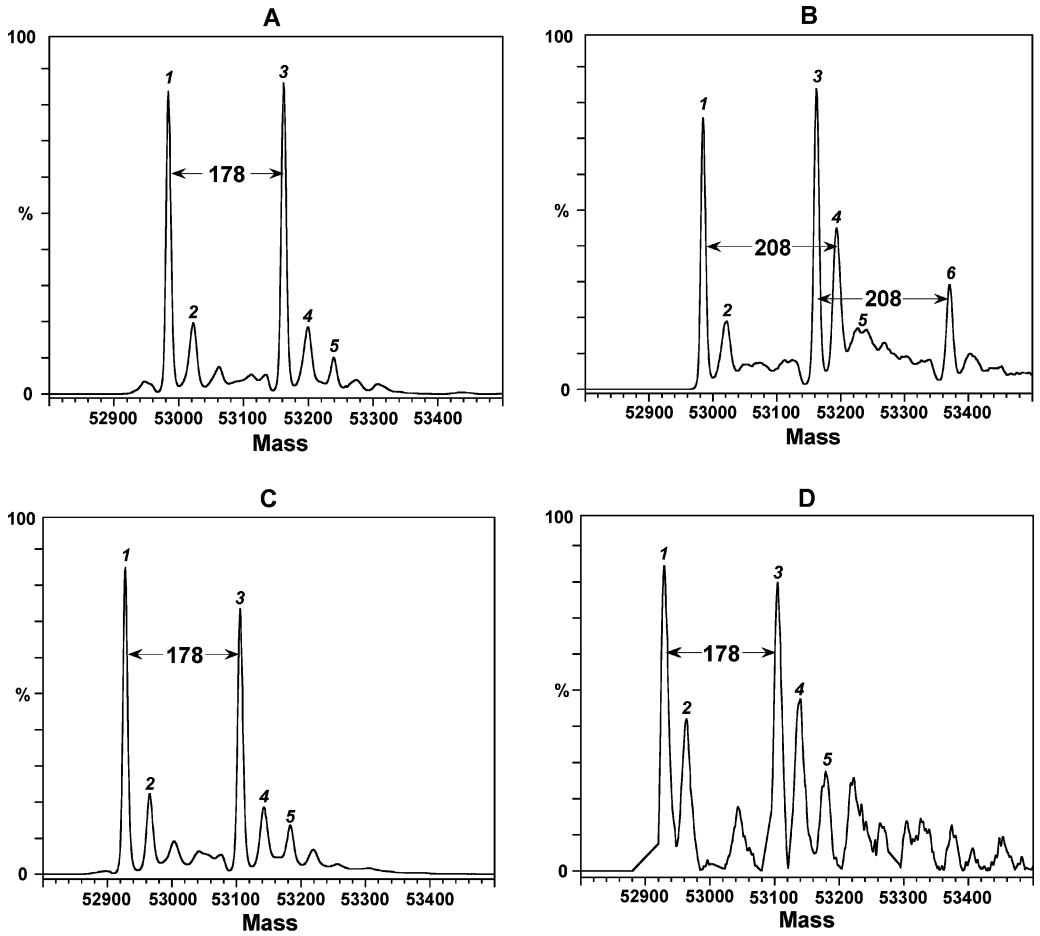

FIGURE 4: Direct detection of the covalent intermediate formed in ADCS-catalyzed reactions. (A) Wild-type ADCS. The peak masses are as follows: peak 1 = 52984.0, peak 2 = 53022.1, peak 3 = 53162.0, peak 4 = 53200.1, and peak 5 = 53239.1 (B) Wild-type ADCS + 2 equiv of chorismate + 0.5 equiv of Mn^{2+} incubated for 5 min. The peak masses are as follows: peak 1 = 52984.7, peak 2 = 53021.5, peak 3 = 53162.2, peak 4 = 53193.8, peak 5 = 53211.4, and peak 6 = 53370.6 (C) K274A. The peak masses are as follows: peak 1 = 52927.6, peak 2 = 52965.5, peak 3 = 53105.7, peak 4 = 53143.6, and peak 5 = 53182.3. (D) K274A + 2 equiv of chorismate + 0.5 equiv of Mn^{2+} incubated for 5 min. The peak masses are as follows: peak 1 = 52927.2, peak 2 = 52965.2, peak 3 = 53104.6, peak 4 = 53143.0, and peak 5 = 53181.5. A mass increase of 208 Da is only seen in the ADCS + chorismate + Mn^{2+} reaction and demonstrates the covalent addition of K274 to chorismate during the course of reaction.

1 and 3 are the two species without potassium while peaks 2, 4, and 5 are their potassium adducts. After incubation of K274A with chorismate and Mn^{2+}, no *new* peaks appeared in the mass spectrum with molecular mass increases of 208 Da due to covalent intermediate formation (Figure 4D).

Difference Spectral Studies of the Covalent Intermediate. The covalent intermediate was detected spectroscopically with UV/vis difference spectra. When chorismate is mixed with ADCS, a new absorption band at 310 nm is observed. The peak is characteristic of C2-substituted chorismate derivatives, e.g., ADIC. The absorption spectra of relevant C2- and C4-substituted compounds are given in the inset to Figure 5. The C2-substituted compounds have a common 310 nm absorption peak that the covalent intermediate displays.

Figure 5 shows the UV/vis spectra of several different reactions. The covalent intermediates formed share the 310 nm peak. Traces 1 and 2 show that, either with or without PabA present, ADCS forms the covalent intermediate without the inclusion of an ammonia source (i.e., glutamine or NH_4^+). It is estimated from the difference spectra that 33% and 22% of ADCS exist as the covalent intermediate in traces 1 and 2, respectively (assuming identical extinction coefficients for the covalent intermediate and ADIC at 310 nm). PabA binding induces a 50% increase in covalent intermediate accumulation. Trace 3 (with PabA) and trace 4 (without PabA) demonstrate that K274A in the presence of chorismate and ammonia gives a spectrally similar intermediate, which was previously shown to be ADIC (*17*). Thus, NH_3 acts to replace the function of K274 in the K274A mutant. Trace 5 (with PabA) and trace 6 (without PabA) show that K274A in the absence of an ammonia source does not form the covalent intermediate with chorismate. DON inactivation of PabA (which mimics the covalent thioester intermediate formed in glutamine hydrolysis) does not enhance formation of the covalent intermediate. Control experiments showed that ADCS incubated either alone or with an ammonia source, K274A (with or without pabA) + chorismate, and K274R (with or without pabA) + chorismate produced no covalent intermediate.

Steady-State Kinetic Analysis in the Absence of Metal Ions. Steady-state k_{cat} values were determined using the PABA fluorescence assay to quantitate the activity of ADCS in the absence of metal ions. The k_{cat} for PabA + ADCS + chorismate + Gln in the absence of metals is 1.14×10^{-4} s^{-1}, and that of ADCS + chorismate + NH_4^+ in the absence of metals is 8.30×10^{-6} s^{-1}.

Pre-Steady-State Kinetic Analysis. Pre-steady-state kinetic analyses of covalent intermediate formation are presented

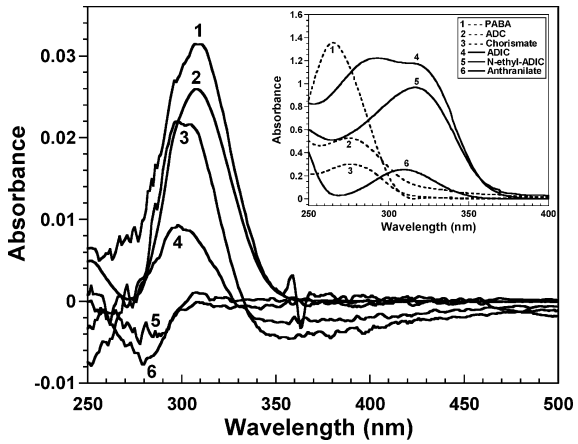

FIGURE 5: Difference spectra of C2-substituted intermediates formed in different ADCS-catalyzed reactions. Traces 1−6 in the main figure represent the following reactions: 1, PabA + ADCS + chorismate; 2, ADCS + chorismate; 3, PabA + K274A + chorismate + NH_4^+; 4, K274A + chorismate + NH_4^+; 5, PabA + K274A + chorismate; 6, K274A + chorismate. The inset gives absorption spectra of compounds involved in this pathway that are grouped by different λ_{max} values. One group presented as dotted lines is C4-substituted compounds whose λ_{max} are below 300 nm. The other group illustrated as solid lines is C2-substituted compounds whose λ_{max} are around 310−320 nm. Traces 1−4 in the main figure show that C2-substituted intermediates exhibit the shared 310 nm absorption. Traces 5 and 6 are negative control reactions.

in Figure 6 and Table 1. The time courses of the reactions were fitted to either one or two exponentials. Data in the absence of an ammonia source fit well to one exponential, while data in the presence of an ammonia source fit well to two exponentials. The observed rate constants for covalent intermediate formation at various chorismate concentrations were fitted to eq 1 to obtain k_{max} and $K_{chorismate}$.

$$k_{obs} = \frac{k_{max}[\text{chorismate}]}{K_{chorismate} + [\text{chorismate}]} \quad (1)$$

The k_{max} for covalent intermediate formation is much larger than the steady-state k_{cat} (at least 160 times larger with PabA and at least 120 times larger without PabA), indicating that this step is not rate-limiting for steady-state turnover. Addition of PabA increases the k_{max} value by approximately 10-fold, independent of the presence of an ammonia source. PabA does not alter $K_{chorismate}$ significantly. Addition of NH_4^+ lowers the k_{max} values approximately 30%, irrespective of the presence of PabA, and also increases $K_{chorismate}$ values approximately 5-fold.

E258 in ADCS Is Crucial for the Covalent Intermediate Formation. Strict conservation in multiple sequence alignments and the active site structure suggest that E258 in ADCS assists covalent intermediate formation by acting as a general acid to protonate the C4 hydroxyl group. The E258A and E258D mutants were made, and their steady-state kinetics were studied. The results are presented in Table 2. The E258A/D-catalyzed reactions are extremely slow. Therefore, high concentrations of enzymes (10−60 μM) and long incubation times (18−24 h with sampling every 2−3 h) were required. The slowest reaction (E258A + PabA + chorismate + Gln) was repeated at three different enzyme concentrations to confirm that observed rates were enzyme dependent. Nonenzymatic background rates were also measured in two control reactions: chorismate + PabA + Gln and chorismate + NH_4^+. Both of these rates are negligible. Compared with wild-type ADCS, the E258A mutant has a k_{cat} value that is 4×10^6-fold lower with PabA + Gln as ammonia source and 2×10^5-fold lower with NH_4^+. The E258D mutant, whose k_{cat} value is 1×10^4-fold lower than wild-type ADCS with PabA + Gln as ammonia source and 3×10^2-fold smaller with NH_4^+ as ammonia source, is remarkably inactive given the small change to the side-chain structure. In contrast to ADCS, the NH_4^+-dependent reactions catalyzed by E258A and E258D are faster than the Gln-dependent reactions.

Addition of acetate rescues the E258A reactions but not the E258D reactions. Due to chorismate inhibition of the E258A/D reactions at high concentrations, 150 μM chorismate was used in the rescue experiments. At this chorismate concentration, acetate increases k_{cat} for E258A + PabA + chorismate + Gln by a remarkable 2×10^4-fold compared to k_{cat} for the same reaction with saturating chorismate in the absence of acetate. Similarly, acetate increases k_{cat} for E258A + chorismate + NH_4^+ by 3×10^3-fold. Difference spectral studies of the E258A/D mutants showed no covalent intermediate formation (data not shown). Addition of acetate to the E258A reaction does not lead to detectable intermediate formation in difference spectra.

HPLC Separation of IS and A213K IS Reaction Mixtures. The A213K mutant of IS was made in an attempt to convert it into an ADCS-like enzyme, with the ability to form a covalent intermediate with chorismate. IS (*entC*) was cloned from *E. coli* BL21(DE3) and overexpressed using a pET28a vector. The His-tagged enzyme was purified to homogeneity by affinity chromatography. K_M and k_{cat} are 4.6 μM and 31.4 min^{-1}, respectively, at 25 °C. These values are in reasonable agreement with previously reported values of $K_M = 14$ μM and $k_{cat} = 173$ min^{-1}at 37 °C (*7*).

HPLC chromatograms for reactions with chorismate as the substrate are shown in Figure 7A. The reaction of wild-type IS with chorismate generated both isochorismate and ADIC in the presence of H_2O and NH_4^+ (trace A). The reaction of the A213K mutant in the absence of NH_4^+ produced isochorismate to a much lesser extent (trace B). When NH_4^+ was added to the A213K reaction, strikingly, there was no ADIC and even less isochorismate formed (trace C). *p*-Hydroxybenzoate (PHB) was the nonenzymatic decomposition product of chorismate, confirmed by control reactions. HPLC chromatograms with ADC as the substrate are shown in Figure 7B. The reaction of IS + ADC + H_2O + NH_4^+ gave the most interesting results (trace A). Besides ADC remaining in the equilibrium mixture, ADIC, isochorismate, chorismate, PABA, and pyruvate were also generated, indicating that IS is capable of catalyzing the fully reversible reaction from ADC to intermediates ADIC and isochorismate and then to chorismate. In contrast to chorismate, ADC was also carried onto PABA by IS by eliminating pyruvate. In the reaction of A213K + ADC + H_2O, only the elimination products PABA and pyruvate were detected (trace B). The reversible pathway leading to ADIC, isochorismate, and chorismate was blocked. Addition of NH_4^+ to this mutant reaction gave no observed differences (trace C). The retention times of ADC and ADIC are known from previous studies (*17*). Isochorismate was identified by ESI-MS using negative ion mode. The identity of the peak marked with a star was

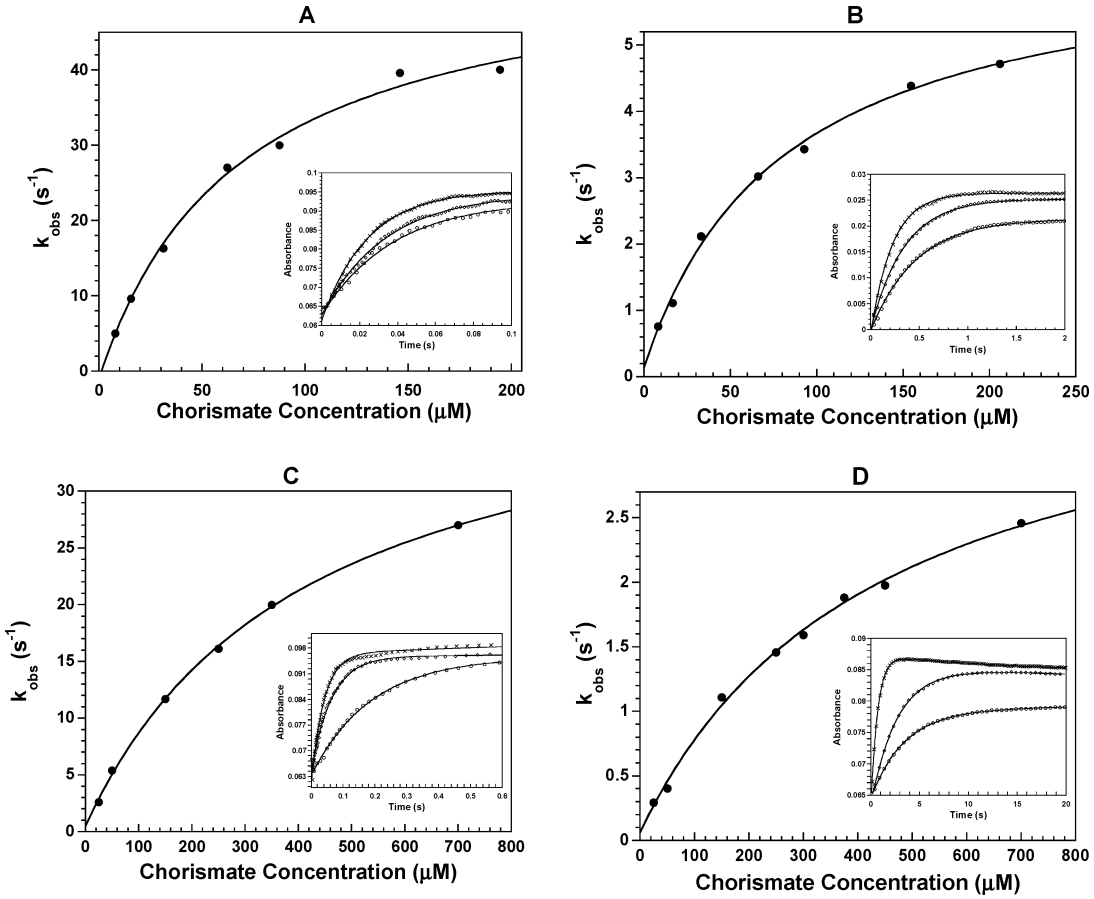

FIGURE 6: Observed rate constants as a function of chorismate concentration for the covalent intermediate formation in (A) PabA + ADCS + chorismate, (B) ADCS + chorismate, (C) PabA + ADCS + chorismate + NH_4^+, and (D) ADCS + chorismate + NH_4^+. In these reactions, the rate constants exhibit hyperbolic dependence on substrate concentration. The solid lines are the best fits to eq 1. Representative absorbance versus time data fitted to exponentials are presented in the insets. Only 10% of the data points are shown, and the solid lines are the best fits obtained from all data points. Chorismate concentrations shown are as follows: inset A, 64 (○), 90 (◇), and 150 (×) μM; inset B, 32 (○), 64 (◇), and 150 (×) μM; inset C, 50 (○), 250 (◇), and 450 (×) μM; inset D, 25 (○), 50 (◇), and 250 (×) μM.

Table 1: Kinetic Constants from Pre-Steady-State Analysis[a]

reaction	k_{max} (s^{-1})	$K_{chorismate}$ (μM)
PabA + ADCS + chorismate	57 ± 3	75 ± 9
ADCS + chorismate	6.3 ± 0.2	71 ± 6
PabA + ADCS + chorismate + NH_4^+	41 ± 1	379 ± 23
ADCS + chorismate + NH_4^+	3.8 ± 0.2	388 ± 39

[a] Assay conditions described in Experimental Procedures were used. 200 mM NH_4^+ was used because a higher concentration of NH_4^+ inhibits NH_4^+-dependent activity of ADCS.

not determined. It is a product of an enzymatic process according to control reactions, but it was not PHB as determined by differences in their fluorescence spectra.

Due to the instability of the A213K mutant in unbuffered water, mass spectral analysis could not be carried out. Thus, no direct evidence for covalent intermediate formation in A213K was obtained. Difference spectral experiments on A213K were also hindered by enzyme instability.

DISCUSSION

Four reaction mechanisms were previously considered as the unifying mechanism for IS, AS, and ADCS (*15*, *16*). The first was a C2 Michael addition followed by C4 elimination in a stepwise sequence via an aci-carboxylate intermediate. The second was a 1,5 S_N2'' concerted addition of nucleophiles to C2 via a Mg^{2+}-bound transition state. The third was covalent catalysis by addition of an enzyme active site nucleophile to C6 of chorismate. The fourth also involved covalent addition to C6 with the carboxylate on the enoylpyruvate side chain of chorismate acting as an intramolecular nucleophile to form a bicyclic lactone intermediate. The available evidence from inhibitor studies precluded C6 addition mechanisms but failed to identify a unifying mechanism for all three enzymes (*16*, *25*).

The ADCS crystal structure suggested K274 as a potential nucleophile (*20*). On the basis of K274 mutant studies, He et al. proposed a unifying mechanism in which IS, AS, and ADCS all initiate their reactions by nucleophilic addition at C2 with different nucleophiles, namely, water in IS, ammonia in AS, and K274 in ADCS (Figure 3). As a result, an enzyme-bound covalent intermediate was proposed for the ADCS-catalyzed reaction (*17*). Recently, ESI-MS detection of a similar covalent adduct of ADCS has been reported using a fluorinated chorismate analogue, providing further evidence for covalent intermediate formation (*19*).

Here, direct detection of the covalent intermediate formed at the ADCS active site was achieved. Since ammonia, which adds to C4 to give the product, is not chemically required for covalent intermediate formation, the intermediate is likely to accumulate and thus be directly detected in the absence

Table 2: Steady-State Kinetic Analysis of E258 Mutants of ADCS

	k_{cat} (s^{-1})		
ammonia source	wild type	E258A	E258D
PabA + Gln	0.53 ± 0.02	$(6.9 \pm 1.2) \times 10^{-8}$ [a,b]	$(2.0 \pm 0.1) \times 10^{-5}$ [a,b]
NH_4^+	0.032 ± 0.002	$(1.7 \pm 0.3) \times 10^{-7}$ [a,b]	$(1.21 \pm 0.02) \times 10^{-4}$ [a,b]
PabA + Gln + acetate		0.0012 ± 0.0001[c]	no rescue[d]
NH_4^+ + acetate		0.00045 ± 0.00007[c]	no rescue[d]

[a] These constants were determined using the discontinuous PABA fluorescence assay. Saturating (1 mM) chorismate, 20 mM Gln, and 200 mM NH_4^+ were used. [b] Nonenzymatic background rates were also measured in two control reactions, chorismate + PabA + Gln and chorismate + NH_4^+ (concentrations are the same as those used in enzymatic reactions), using the PABA fluorescence assay. The background rates are negligible. [c] Acetate rescue reaction kinetic constants were determined by varying acetate concentration at fixed chorismate and ammonia source concentrations using LDH assay. 150 μM chorismate was used instead of 1 mM since a higher concentration of chorismate inhibits E258A/D when acetate is present. Ammonia source concentrations remained the same. $K_{acetate}$ for E258A + chorismate + PabA + Gln + acetate is 214 ± 47 mM, and $K_{acetate}$ for E258A + chorismate + NH_4^+ + acetate is 412 ± 116 mM. [d] Acetate rescue was not detected in E258D reactions using the LDH assay. 150 μM chorismate was used.

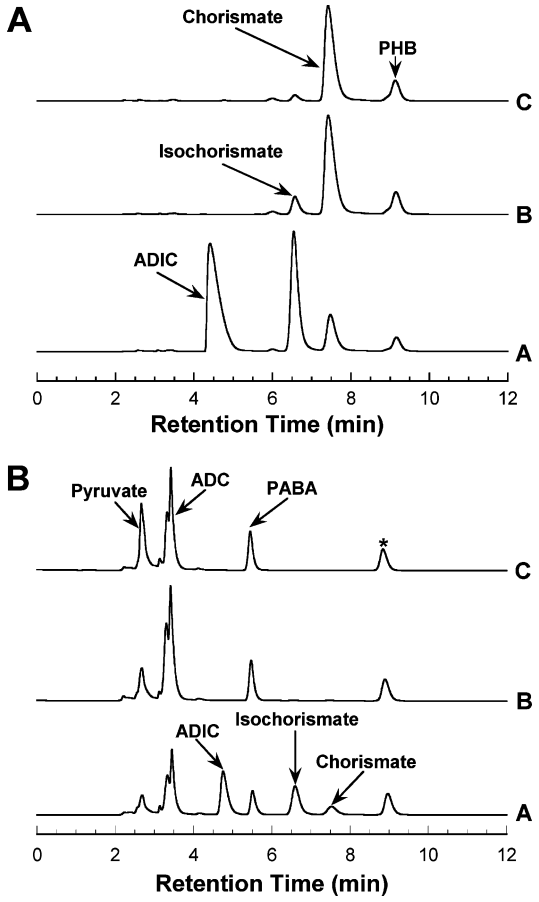

FIGURE 7: (A) HPLC chromatograms of reaction mixtures catalyzed by IS or its mutant A213K with chorismate as the substrate. The figure labels indicate the following: A, IS + chorismate + H_2O + NH_4^+; B, A213K + chorismate + H_2O; C, A213K + chorismate + H_2O + NH_4^+. (B) HPLC chromatograms of reaction mixtures catalyzed by IS or its mutant A213K when ADC was the substrate. The figure labels indicate the following: A, IS + ADC + H_2O + NH_4^+; B, A213K + ADC + H_2O; C, A213K + ADC + H_2O + NH_4^+.

of an ammonia source. The ESI-MS results clearly show that ADCS mixed with chorismate shows a 208 Da mass increase, the predicted mass increase due to covalent intermediate formation. The K274A mutant did not produce the modified species under the same conditions. This conclusively demonstrates the formation of a covalent intermediate in the ADCS-catalyzed reaction. A recently published study presented similarly convincing evidence for covalent intermediate formation (*26*).

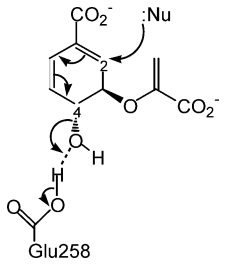

FIGURE 8: Mechanism of C4 hydroxyl cleavage facilitated by E258 during the formation of the covalent intermediate in ADCS.

The spectral properties of the covalent intermediate were also characterized. The compounds under consideration fall into two groups based on their spectral properties. ADC and chorismate are C4-substituted cross-conjugated compounds whose λ_{max} are below 300 nm. In contrast, ADIC and *N*-ethyl-ADIC are fully conjugated with the carboxylate group and show λ_{max} values between 310 and 320 nm. By analogy to ADIC, the covalent intermediate is predicted to absorb predominantly in the 310−320 nm region. This proved to be the case. When chorismate was mixed with ADCS, a peak at 310 nm was rapidly generated in difference spectra. Additional experiments showed that the presence of both chorismate and ADCS is necessary and sufficient for formation of the 310 nm peak. PabA and different ammonia sources were optional. Moreover, the K274A mutant of ADCS combined with an ammonia source also gave the 310 nm peak, which is expected to be ADIC instead of the covalent intermediate.

The identity of the 310 nm peak as the covalent intermediate formed in ADCS reactions was further confirmed by the following observations. First, the intensity of the 310 nm peak was reduced approximately 2-fold when the ADCS concentration was reduced from 10 to 5 μM, demonstrating that it was an enzymatic species. Second, addition of PabA increased the intensity of the 310 nm peak, reflecting the known fact that PabA binding enhances ADCS reactivity. Third, the inclusion of ammonia sources in the reaction (either NH_4^+ or Gln) decreased the intensity of the 310 nm peak, presumably by carrying it forward in the reaction sequence and thereby depleting it. Fourth, on coupling with excess ADCL in the presence of ammonia sources, the 310 nm peak was not observed. This demonstrates reversible covalent intermediate formation and rapid equilibration with ADC. Fifth, the 310 nm peak was not formed when metal ions were excluded.

The pre-steady-state kinetics of covalent intermediate formation were measured at 310 nm in a stopped-flow spectrometer. The reaction of PabA + ADCS + chorismate shows that the covalent intermediate is indeed formed in a kinetically competent manner ($k_{max} = 57\ s^{-1}$) since the k_{cat} under similar conditions with Gln as a nitrogen source is $0.53\ s^{-1}$ (*17*). Similarly, the ADCS + chorismate reaction forms the covalent intermediate in a kinetically competent manner since $k_{max} = 6.3\ s^{-1}$ is significantly faster than $k_{cat} = 0.032\ s^{-1}$ under similar conditions with NH_4^+ as the nitrogen source. These results also provide strong evidence that the rate-limiting step occurrs after formation of the covalent intermediate. PabA significantly increases both the k_{max} values for covalent intermediate formation and the steady-state k_{cat} values presumably by binding ADCS tightly and enforcing a more reactive conformation. The $K_{chorismate}$ values in either the absence or presence of NH_4^+ are significantly higher in the pre-steady-state kinetics, suggesting that there is a significant forward commitment for the covalent intermediate in the steady state once it is formed.

Multiple sequence alignment and active site modeling studies show that E258 in ADCS is completely conserved in AS, IS, and ADCS. It is well positioned to protonate the C4 hydroxyl group of chorismate, thereby making it a better leaving group. To test this hypothesis, E258A and E258D were studied. The E258A-catalyzed reaction is 4×10^6-fold slower than that catalyzed by wild-type ADCS when PabA + Gln are the ammonia source and 2×10^5-fold slower when NH_4^+ is the ammonia source.

E258D was expected to be, and is, more active than E258A since it retains an acidic functional group that can protonate the C4 hydroxyl. The E258D-catalyzed reaction is 1×10^4-fold slower than that catalyzed by wild-type ADCS when PabA + Gln are the ammonia source and 3×10^2-fold slower when NH_4^+ is the ammonia source.

Acetate dramatically rescues E258A-catalyzed reactions (2×10^4-fold for E258A + PabA + chorismate + Gln, 3×10^3-fold for E258A + chorismate + NH_4^+). However, it does not rescue those catalyzed by E258D. This is likely due to the larger and negatively charged aspartate side chain in E258D preventing the access of acetate to the C4 hydroxyl group. Acetate-rescued E258A reactions have faster rates for PabA + Gln-dependent reactions than for NH_4^+-dependent reactions, reminiscent of the results with wild-type ADCS. This suggests that acetate functionally replaces E258 and facilitates the cleavage of the C4 hydroxyl by general acid catalysis. Difference spectra showed no indication of covalent intermediate accumulation in the E258A/D-catalyzed reactions. The above evidence demonstrates the crucial role that E258 plays as a general acid/base catalyst for facilitating the departure of the C4 hydroxyl in covalent intermediate formation in ADCS.

Unlike ADCS, IS and AS do not form a covalent intermediate since they employ water and ammonia, respectively, as nucleophiles. Correspondingly, the amino acid at position 274 is alanine in both of these enzymes. Mutation of A274 to Lys in IS and AS could potentially enable them to form the covalent intermediate as in the ADCS reaction. The IS mutant A213K was therefore studied. HPLC analyses of wild-type IS and A213K provide circumstantial evidence for the formation of covalent intermediates between K213 in the mutant and chorismate or ADC. In Figure 7A, when chorismate was used as the substrate, both isochorismate and ADIC were generated in the IS + chorismate + H_2O + NH_4^+ reaction. Strikingly, no ADIC was generated in the same reaction catalyzed by A213K. The amount of isochorismate generated was also sharply reduced in A213K-catalyzed reactions. This is consistent with K213 in the mutant enzyme forming a covalent adduct with C2 as in ADCS, thus blocking the formation of ADIC and isochorismate. Nevertheless, simple steric hindrance by K213 cannot be ruled out. Similarly, the A213K mutant showed altered reaction specificity when ADC was used as substrate (Figure 7B). In reactions containing IS + ADC + H_2O + NH_4^+, the elimination reaction products PABA and pyruvate and the reversible reaction products ADIC, isochorismate, and chorismate were detected. Remarkably, in reactions containing A213K + ADC + H_2O and A213K + ADC + H_2O + NH_4^+, only elimination products, whose production was unlikely to be affected by the A213K mutation, were detected. The products expected from reversible reactions involving K213 addition to C2 of chorismate were not detected, which is most likely due, in our opinion, to formation of the covalent intermediate between K213 and C2 but can also be explained by steric hindrance without formation of a covalent intermediate.

REFERENCES

1. Hanson, A. D., and Roje, S. (2001) One-Carbon Metabolism in Higher Plants, *Annu. Rev. Plant Physiol. Plant Mol. Biol. 52*, 119−137.
2. Stanger, O. (2002) Physiology of Folic Acid in Health and Disease, *Curr. Drug Metab. 3*, 211−223.
3. Ye, Q. Z., Liu, J., and Walsh, C. T. (1990) *p*-Aminobenzoate Synthesis in *Escherichia coli*: Purification and Characterization of Pabb as Aminodeoxychorismate Synthase and Enzyme X as Aminodeoxychorismate Lyase, *Proc. Natl. Acad. Sci. U.S.A. 87*, 9391−9395.
4. Nichols, B. P., Seibold, A. M., and Doktor, S. Z. (1989) Para-Aminobenzoate Synthesis from Chorismate Occurs in Two Steps, *J. Biol. Chem. 264*, 8597−8601.
5. Green, J. M., and Nichols, B. P. (1991) *p*-Aminobenzoate Biosynthesis in *Escherichia coli*. Purification of Aminodeoxychorismate Lyase and Cloning of Pabc, *J. Biol. Chem. 266*, 12971−12975.
6. Romero, R. M., Roberts, M. F., and Phillipson, J. D. (1995) Anthranilate Synthase in Microorganisms and Plants, *Phytochemistry 39*, 263−276.
7. Liu, J., Quinn, N., Berchtold, G. A., and Walsh, C. T. (1990) Overexpression, Purification, and Characterization of Isochorismate Synthase (Entc), the First Enzyme Involved in the Biosynthesis of Enterobactin from Chorismate, *Biochemistry 29*, 1417−1425.
8. Blanc, V., Gil, P., Bamas-Jacques, N., Lorenzon, S., Zagorec, M., Schleuniger, J., Bisch, D., Blanche, F., Debussche, L., Crouzet, J., and Thibaut, D. (1997) Identification and Analysis of Genes from *Streptomyces pristinaespiralis* Encoding Enzymes Involved in the Biosynthesis of the 4-Dimethylamino-L-Phenylalanine Precursor of Pristinamycin I, *Mol. Microbiol. 23*, 191−202.
9. McDonald, M., Mavrodi, D. V., Thomashow, L. S., and Floss, H. G. (2001) Phenazine Biosynthesis in Pseudomonas Fluorescens: Branchpoint from the Primary Shikimate Biosynthetic Pathway and Role of Phenazine-1,6-Dicarboxylic Acid, *J. Am. Chem. Soc. 123*, 9459−9460.
10. Pelludat, C., Brem, D., and Heesemann, J. (2003) Irp9, Encoded by the High-Pathogenicity Island of Yersinia Enterocolitica, Is Able to Convert Chorismate into Salicylate, the Precursor of the Siderophore Yersiniabactin, *J. Bacteriol. 185*, 5648−5653.
11. Davidson, B. E. (1987) Chorismate Mutase-Prephenate Dehydratase from *Escherichia coli*, *Methods Enzymol. 142*, 432−439.
12. Holden, M. J., Mayhew, M. P., Gallagher, D. T., and Vilker, V. L. (2002) Chorismate Lyase: Kinetics and Engineering for Stability, *Biochim. Biophys. Acta 1594*, 160−167.

13. Dosselaere, F., and Vanderleyden, J. (2001) A Metabolic Node in Action: Chorismate-Utilizing Enzymes in Microorganisms, *Crit. Rev. Microbiol. 27*, 75−131.
14. Roberts, F., Roberts, C. W., Johnson, J. J., Kyle, D. E., Krell, T., Coggins, J. R., Coombs, G. H., Milhous, W. K., Tzipori, S., Ferguson, D. J., Chakrabarti, D., and McLeod, R. (1998) Evidence for the Shikimate Pathway in Apicomplexan Parasites, *Nature 393*, 801−805.
15. Walsh, C. T., Liu, J., Rusnak, F., and Sakaitani, M. (1990) Molecular Studies on Enzymes in Chorismate Metabolism and the Enterobactin Biosynthetic Pathway, *Chem. Rev. 90*, 1105−1129.
16. Kozlowski, M. C., Tom, N. J., Seto, C. T., Sefler, A. M., and Bartlett, P. A. (1995) Chorismate-Utilizing Enzymes Isochorismate Synthase, Anthranilate Synthase, and *p*-Aminobenzoate Synthase—Mechanistic Insight through Inhibitor Design, *J. Am. Chem. Soc. 117*, 2128−2140.
17. He, Z., Stigers Lavoie, K. D., Bartlett, P. A., and Toney, M. D. (2004) Conservation of Mechanism in Three Chorismate-Utilizing Enzymes, *J. Am. Chem. Soc. 126*, 2378−2385.
18. Morollo, A. A., and Bauerle, R. (1993) Characterization of Composite Aminodeoxyisochorismate Synthase and Aminodeoxyisochorismate Lyase Activities of Anthranilate Synthase, *Proc. Natl. Acad. Sci. U.S.A. 90*, 9983−9987.
19. Bulloch, E. M., Jones, M. A., Parker, E. J., Osborne, A. P., Stephens, E., Davies, G. M., Coggins, J. R., and Abell, C. (2004) Identification of 4-Amino-4-Deoxychorismate Synthase as the Molecular Target for the Antimicrobial Action of (6s)-6-Fluoroshikimate, *J. Am. Chem. Soc. 126*, 9912−9913.
20. Parsons, J. F., Jensen, P. Y., Pachikara, A. S., Howard, A. J., Eisenstein, E., and Ladner, J. E. (2002) Structure of *Escherichia coli* Aminodeoxychorismate Synthase: Architectural Conservation and Diversity in Chorismate-Utilizing Enzymes, *Biochemistry 41*, 2198−2208.
21. Roux, B., and Walsh, C. T. (1992) *p*-Aminobenzoate Synthesis in *Escherichia coli*: Kinetic and Mechanistic Characterization of the Amidotransferase Paba, *Biochemistry 31*, 6904−6910.
22. Anderson, K. S., Kati, W. M., Ye, Q. Z., Liu, J., Walsh, C. T., Benesi, A. J., and Johnson, K. A. (1991) Isolation and Structure Elucidation of the 4-Amino-4-Deoxychorismate Intermediate in the Paba Enzymatic Pathway, *J. Am. Chem. Soc. 113*, 3198−3200.
23. Teng, C. P., Ganem, B., Doktor, S. Z., Nichols, B. P., Bhatnagar, R. K., and Vining, L. C. (1985) Total Synthesis of (±)-4-Amino-4-Deoxychorismic Acid: A Key Intermediate in the Biosynthesis of *p*-Aminobenzoic Acid and L-(*p*-Aminophenyl)Alanine, *J. Am. Chem. Soc. 107*, 5008−5009.
24. Geoghegan, K. F., Dixon, H. B., Rosner, P. J., Hoth, L. R., Lanzetti, A. J., Borzilleri, K. A., Marr, E. S., Pezzullo, L. H., Martin, L. B., LeMotte, P. K., McColl, A. S., Kamath, A. V., and Stroh, J. G. (1999) Spontaneous Alpha-N-6-Phosphogluconoylation of a "His Tag" in *Escherichia coli*: The Cause of Extra Mass of 258 or 178 Da in Fusion Proteins, *Anal. Biochem. 267*, 169−184.
25. Walsh, C. T., Erion, M. D., Walts, A. E., Delany, J. J., III, and Berchtold, G. A. (1987) Chorismate Aminations: Partial Purification of *Escherichia coli* Paba Synthase and Mechanistic Comparison with Anthranilate Synthase, *Biochemistry 26*, 4734−4745.
26. Bulloch, E. M., and Abell, C. (2005) Detection of Covalent Intermediates Formed in the Reaction of 4-Amino-4-Deoxychorismate Synthase, *ChemBioChem 6*, 832−834.

BI052216P